P7.4 WIND STRESS AND STRESS CURL FROM AIRCRAFT MEASUREMENTS AND THEIR CONNECTION TO LOCAL COASTAL UPWELLING

Qing Wang[1*], John Kalogiros[2], Steve Ramp[1], Jeff Paduan[1], Gintas Buzorius[1] and Haf Jonsson[1]
[1]Naval Postgraduate School, Monterey, California
[2]National Observatory of Athens, Athens, Greece

1. INTRODUCTION

Wind stress is an important forcing of sea surface perturbations either as waves or as surface currents and drives coastal upwelling through two processes: Ekman transport and Ekman pumping. Ekman transport is due to a uniform wind stress field, while Ekman pumping is a result of the divergence of Ekman transport, or equivalently, the curl of wind stress (Kraus and Businger 1994). Along the west coast of major continents in the northern hemisphere, such as the coastal California region, northerly winds along the coast favor coastal upwelling through Ekman transport while positive stress curl is expected to enhance upwelling locally through Ekman pumping. The focus of this work is on the latter: upwelling through positive wind stress curl.

The large scale wind stress field over the ocean is usually estimated indirectly from buoy or shipboard measurements (Winant and Dorman 1997) or atmospheric models (Tjernström and Grisogono 2000; Pickett and Paduan 2003). Aircraft turbulence measurements have also been used to map the coastal near surface wind stress field during several field experiments in the past (Enriquez and Friehe 1995; Rogers et al. 1998; Dorman et al. 2000; Ström et al. 2001; Brooks et al. 2003). However, a systematic study of the effect of wind stress curl on local upwelling using observations has not been performed.

2. MEASUREMENTS AND DATA PROCESSING

During AOSN-II project, about forty flights were carried out in the area of Monterey Bay with the Twin Otter research aircraft operated by the Center for Interdisciplinary Remotely Piloted Aircraft Study (CIRPAS) of the Naval Postgraduate School (NPS) between January 2003 and February 2004 with an intensive observational period (IOP) in August 2003. Figure 1 shows a typical flight pattern that usually includes a low-level 'lawn-mowing' flight pattern close to the coastline, slant path and spiral soundings at the northern and southern ends of the flight track, and a long alongshore leg at 35 m altitude in the offshore region. The lawnmower pattern is done for near surface sampling close to the coast. Results from this section of the flight are of most interest in this paper. Thirty three AOSN-II flights included the dense 'lawn-mowing' flight pattern at 30-40 m above sea surface as well as soundings at the northern and southern parts of the measurement area (Fig. 1) at an average airspeed of 55 m s^{-1}. Data from these flights were used to examine the horizontal distribution of various meteorological quantities including SST from an infrared radiometric thermometer. Additional measurements used in this work include sea surface current from the local CODAR HF radar network (Paduan and Rosenfeld 1996) and ocean profiles from the Monterey Bay Aquarium Research Institute (MBARI) moorings.

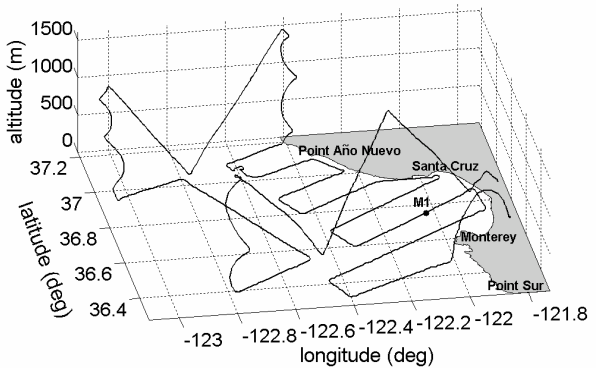

Figure 1. A typical flight track of Twin Otter in the area of Monterey Bay (August 11, 2003). M1 is the MBARI buoy located in the center of the bay.

Turbulence measurements (10 Hz) were obtained with a radome probe and fast temperature and humidity sensors (Kalogiros and Wang 2002) and turbulence fluxes were calculated with the eddy correlation method using a horizontal averaging length of 5 km. This averaging length selection was based on spectral analysis results. Wind stress curl is estimated as:

$$\nabla \times \tau = \frac{\partial \tau_y}{\partial x} - \frac{\partial \tau_x}{\partial y}, \qquad (1)$$

where x and y are the east and north directions, respectively. The estimates of stress components τ_x and τ_y are first interpolated linearly onto a regular grid in the area of measurements with 5 km resolution. A 15 km×15 km area averaging is

* *Corresponding author address:* Qing Wang, Naval Postgraduate School, Monterey, CA 93943; e-mail: qwang@nps.edu.

also applied before calculating the required gradients of stress components using the centered difference scheme. This way, a smooth variation of wind stress curl is estimated that retains the variations at scales larger than 15 km and with sufficient accuracy as discussed below. A detailed measurement and sampling error analysis showed that the average wind stress curl error ranged from 0.15 Nm^{-2}/100 km to 0.25 Nm^{-2}/100 km. The error due to non-stationary effects on wind stress curl was quite smaller. This total error is sufficiently low for our purposes and is achieved after adequate smoothing of the stress field at the cost of losing spatial resolution and systematically smoothing out extreme characteristics (i.e. small scales) of the wind stress curl field.

3. TYPICAL FLOW PATTERNS

The AOSN-II measurements were made under a variety of large-scale wind conditions that can be generalized into four basic categories based on mean wind direction. Table 1 summarizes the wind speed and direction of each category as well as a few subcategories frequently observed during the thirty three flights used in this study.

Table 1. Area averaged wind speed and direction for each category of near sea surface atmospheric flow in the measurement region. U and dir are wind speed and direction, respectively.

Flow category	# (no)	U ($m\ s^{-1}$)	dir (deg)
northerly wind	21	2.0-17.1	301-360
acceleration	11	3.3-15.0	303-350
expansion fan	3	10.3-15.0	317-334
southerly surge	3	2.0-3.7	301-360
southerly	4	4.9-16.7	152-154
easterly offshore	4	4.2-5.2	28-98
westerly onshore	4	2.3-5.7	230-269
southerly surge	1	5.5	238

The basic categories are defined based on average wind direction (along or cross the average California coastline at the direction of 315^o). The subcategories are identified based on specific characteristics of the atmospheric flow such as wind acceleration at the northern part of Monterey Bay with possible expansion fan or southerly surge south of the bay. The typical wind flow conditions, especially during summer, at the California coast are north-northwesterly wind (NNW) along the coast which intensifies offshore due to the persistent high pressure system over the eastern Pacific Ocean. Significant channeling effects were observed when average wind speed was high (greater than 10 ms^{-1}) and the wind direction is along the coastline. Southerly surges only occurred in a small part of the measurements area and, thus, they were incompletely sampled. Southerly wind directions were observed during the summer in short breaks of the dominant northerly wind conditions. Easterly offshore flow was observed during the wintertime that brought the cold air from inland. The cases of westerly wind were from days with local thermal circulation (sea-breeze) when the synoptic scale wind was weak.

3.1 *Northerly wind*

North-north-westerly wind along the coast was the most frequently observed flow pattern during AOSN-II. Such wind conditions prevailed between 6 and 19 August, 2003, during which four Twin Otter flights were made in four nearly consecutive days (10, 11, 13, and 15, August 2003) and at about the same time of day (morning to noon). There were no obvious flow changes in wind data of NDBC buoy from 6 to 19 August 2003. Figure 2 provides an averaged view of the spatial distribution of the various quantities using the measurements from the four flights. This averaging process allows us to retain the persistent features similar to averaging simple time series of measurements.

Moderate acceleration of the wind is observed in a limited region just north of the bay. This acceleration is probably not significant enough to be considered a major wind speed maximum like in the case of supercritical flow and expansion fan (Winant et al. 1988). However, an increase in wind stress associated with the relatively high wind region at (36.9 N, -122.4 E), where wind stress increased from near 0 to over 0.1Nm^{-2} in the along wind direction and also far offshore can be identified. Inside Monterey bay, wind stress decreases towards the coast in response to the reduction of wind speed. According to vertical cross sections of the atmospheric structure constructed from sawtooth aricraft soundings (not shown here) this was due to wind sheltering by the coastal mountains. The weak wind forcing leads to shallow surface mixed layer and hence a warm patch of SST due to solar heating.

In addition, the increased atmospheric stability in areas of low SST, such as in the upwelling region of Point Año Nuevo to the north of the bay, is likely another reason for the decreased wind stress close to the coast (Enriquez and Friehe 1997). Discrepancies

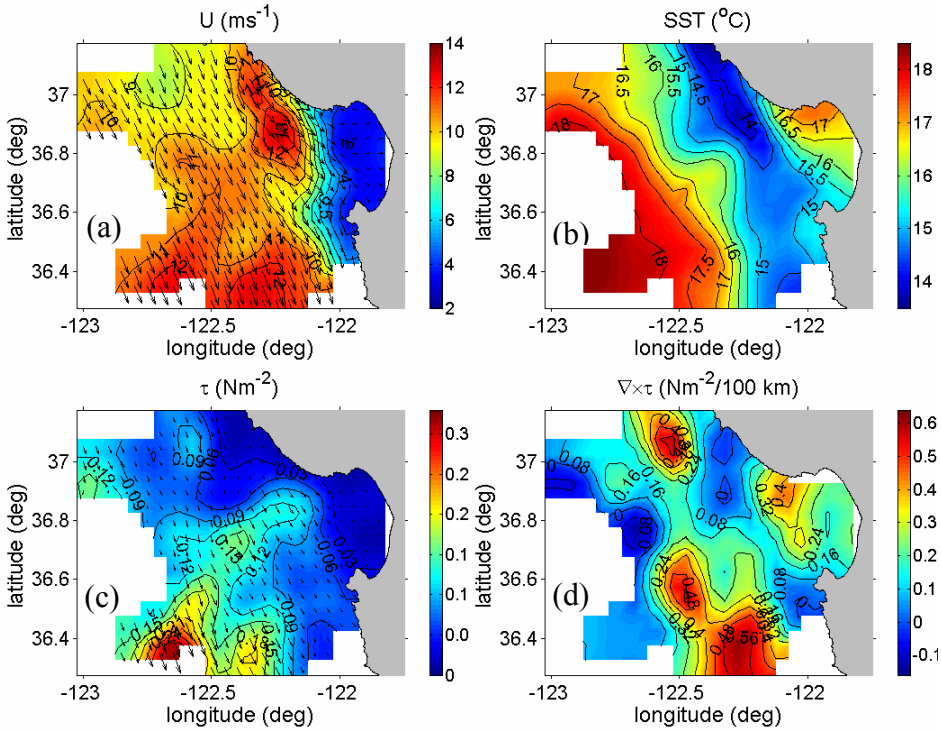

Figure 2. Spatial distribution of (a) wind speed (U), (b) SST, (c) wind stress (τ), and (d) wind stress curl (∇ x τ) estimated from aircraft legs at about 35 m above sea level. The results were averaged from four aircraft flights on 10, 11, 13, and 15 August, 2003 (from about 0915 to 1230 LST) under northerly wind conditions. All flights included in this figure used nearly the same flight pattern as that in Fig. 1.

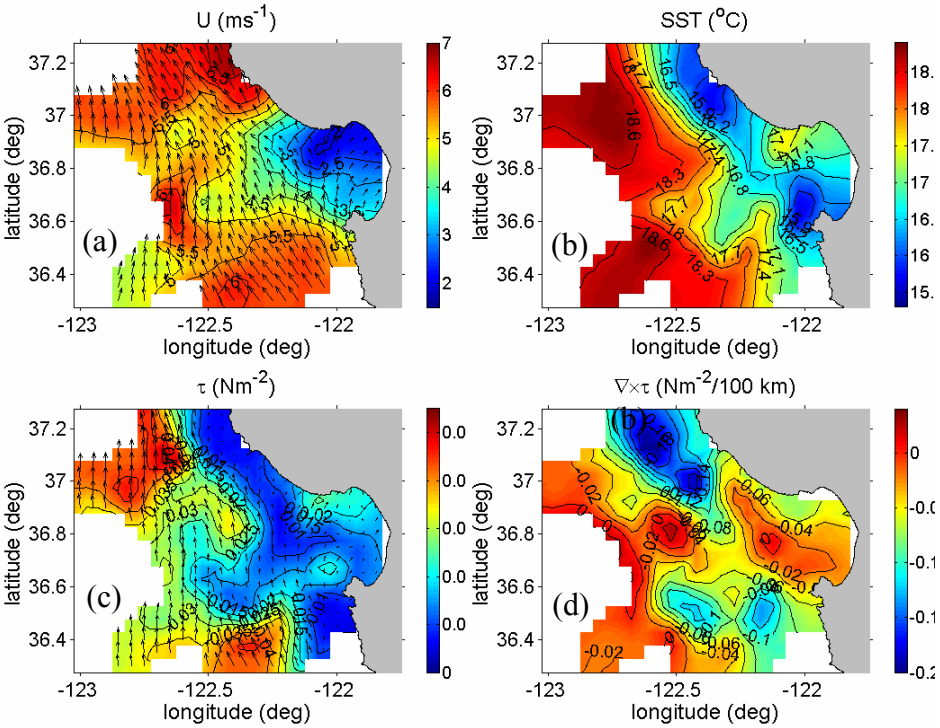

Figure. 3. Same as in Fig. 2, except for flights on 20, 21 and 22 of August, 2003 (from about 0930 to 1300 LST) under southerly wind conditions.

between winds speed and wind stress fields may be observed in enhanced upwelling areas due to non-stationary and non-homogeneity effects (Ström et al. 2001). Furthermore, sea state, and in particular the frequent swell occurrence in the area, may have significant effects on drag coefficient, i.e. wind stress (Geernaert et al. 1986;Donelan et al. 1993; and Drennan et al., 2003).

Wind stress curl may result in local upwelling and hence reduced SST. However, the effect of wind stress curl in the coastal zone may be reduced and spread over a broader area than far offshore as discussed by Enriquez and Friehe (1995) or masked by background upwelling due to northerly winds which favor Ekman transport (Tjernström and Grisogono 2000). As a result, in some cases of AOSN-II, the effect of upwelling due to Ekman pumping on SST is in fact secondary to other processes like SST advection as in the case shown in Fig. 2. Figure 2 shows that the general reduction of wind stress towards the coast under northerly winds leads to an average positive wind stress curl up to 0.6 Nm^{-2}/100 km. However, wind stress curl pattern is complex due to the spatial variability of wind stress field described above with small local maxima where the curl becomes zero. In areas of maximum positive wind stress curl, no reduction of SST is observed, suggesting that the small scale details of the stress curl pattern do not correlate with the SST pattern. On the contrary, the wind stress curl is the smallest at the Point Año Nuevo area of cold SST and its southwards extension. The maximum wind speed in this area suggests SST advection by sea surface current being a dominant factor, a result also shown by Ramp et al. (2005).

3.2 *Southerly wind*

The flow characteristics of the southerly wind conditions are illustrated in Fig. 3 using the average of the observations in three successive southerly wind cases from 20 to 22 of August, 2003, which was a break between the usually northerly winds during summer. Compared to the northerly wind condition in the previous case (Fig. 2), wind speed is smaller (note different color schemes are used for Figs. 2 and 3) and is not as variant except for the reduction in the bay due to upstream blocking from the Santa Cruz mountains to the north of the bay. Wind stress is also small in magnitude and shows more variability than wind speed which can be explained as reduced level of turbulence mainly due to increased atmospheric stability in areas of low SST. Thus, there is a zone of low turbulence and low wind stress close to the shore. Under southerly winds such stress field should give negative wind stress curl, which is indeed observed in spite of the small magnitude compared to that in the northerly wind events. The cold SST center at Point Año Nuevo to the north of the bay is weaker, but still evident despite that the southerly wind is not favorable for upwelling. Apparently, the peak of negative wind stress curl and a cool SST center near Point Año Nuevo indicates that the potential warming of SST due to down-welling from the negative stress curl is not large enough to offset the existing cool SST center previously generated during the northerly wind events. In addition, an area of low SST can be seen at the southern edge of the bay just offshore of the Monterey Peninsula. This is probably due to advection of cold water from the southern upwelling center at Point Sur to the south of the bay.

Analysis of less frequent onshore (sea breeze) or offshore (cold air outflow during winter) wind conditions (not shown here) showed that in these cases a small but significant local maximum of wind and wind stress develops at the mouth of Monterey Bay. This wind stress peak results in a well organized and coherent wind stress curl pattern with an extended area of positive values (0.1-0.2 Nm^{-2}/100 km) at the north (south) part of the bay during onshore (offshore) wind in favor of local upwelling. Local upwelling could be observed in the SST pattern.

4. SEA SURFACE CURRENTS AND SST ADVECTION

According to the above discussion correlation between wind stress curl and local SST changes (e.g. SST reduction under positive wind stress curl) was not evident for the northerly or the southerly wind conditions. In fact, in both the northerly and southerly wind cases wind turbulence pattern was complex with significant small scale variations and a reduced magnitude in the areas of low SST probably due to the stable thermal stratification in the atmospheric surface layer. Thus, we conclude that horizontal advection should be the most significant factor controlling the SST field under these conditions.

Figure 4 shows the correlation of SST depression between the values far offshore and in the near shore zone and alongshore current defined as the component of sea surface current parallel to the average coastline direction. The near shore coastal upwelling zone was defined by the baroclinic oceanic Rossby radius of deformation (about 20 km from the coastline). The

sea surface current values used in Fig. 4 are 4 hour averages of CODAR measurements available only in the area of Monterey Bay during each flight. Filled circles are from flights in northerly wind conditions with acceleration or expansion fan (see Table 1) and average wind speed above 5 m s^{-1}.

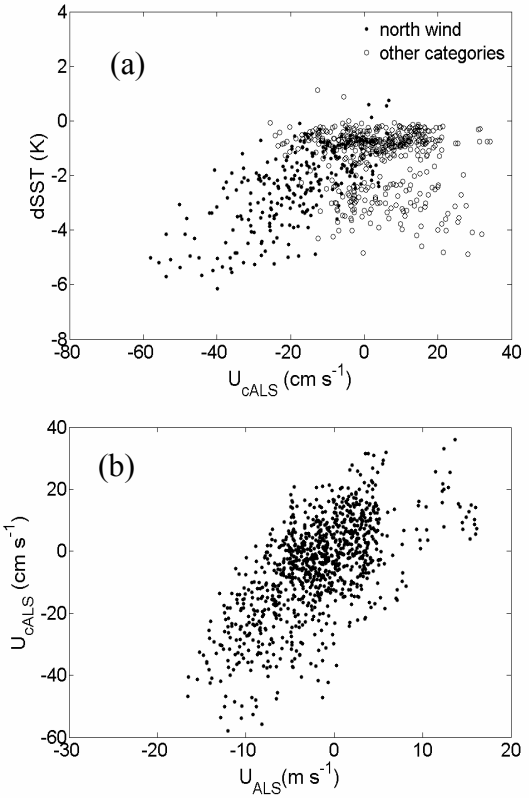

Figure 4. (a) Correlation of the SST depression (dSST) with the component of sea surface current along the average direction of the coastline at about 315^{o} (U_{cALS}); and (b) correlation of U_{cALS} with the corresponding component of wind speed along the same direction (U_{ALS}).

The correlation of SST with sea surface current is clear for the northerly wind conditions, suggesting advection of colder SST from the upwelling area to the north of Monterey Bay. Significant scatter is seen for other wind categories dominated by southerly wind condition with weak surface currents and a vague opposite trend (possible advection of colder SST from the area to the south of the bay). This component of sea surface current along the coastline is well correlated with the corresponding wind component (Fig. 4b), suggesting the dominant role of the wind forcing on upwelling and SST.

5. LOCAL UPWELLING DUE TO EKMAN PUMPING

In this section, we show results from July 13, 2003 when lower SST areas was clearly a result of Ekman pumping. Figure 5 presents the horizontal distribution of relevant meteorological quantities from this flight. This figure show that on that day there was rapid acceleration of wind speed accompanied by wind direction change and a significant and fast reduction of boundary layer height (inferred from near-surface air pressure not shown here) at the turn of the coastline at the north of Monterey Bay, which are characteristics of an expansion fan originating from Point Año Nuevo.

The center of wind stress maximum is located slightly to the south of the peak wind speed (Fig. 5c). A well defined center of the positive wind stress curl is also apparent with maximum stress curl exceeding 1 N m^{-2}/100 km at the mouth of the bay. Measurements from the MBARI buoy (M1) located at the center of the bay are shown in Fig. 6. Rapid cooling of the upper 20 m of the ocean appears to start after 1200 LST, when the wind speed increased to more than 6 ms^{-1} and the flight on 13th of July took place. Probably the value of the peak positive stress curl was much reduced (or absent) earlier in the morning when wind speed was much lower. A delayed response (probably a couple of hours for the scale of the upwelling event of these days) of the ocean to the wind forcing also is expected. On July 13, 2003, the day when the aircraft observed the presence of the expansion fan, there was the shallower ocean surface layer and the most significant cooling of the three consecutive days presented in Fig. 6. Since the SST field is warmer in the upwind region at Point Año Nuevo (Fig. 5b), the cooling of the upper water at the M1 buoy location cannot be a result of horizontal advection. The cooling has hence resulted from upwelling caused by the significant positive stress curl (Ekman pumping) at the mouth of Monterey Bay (Fig. 5d).

6. CONCLUSIONS

Aircraft turbulence data from AOSN-II campaign were used to study the effect of sub-mesoscale wind stress curl on coastal upwelling through Ekman pumping in the area of Monterey Bay. Wind stress curl involves estimating the difference of spatial gradients of a turbulence quantity (wind stress) and, thus, is difficult to

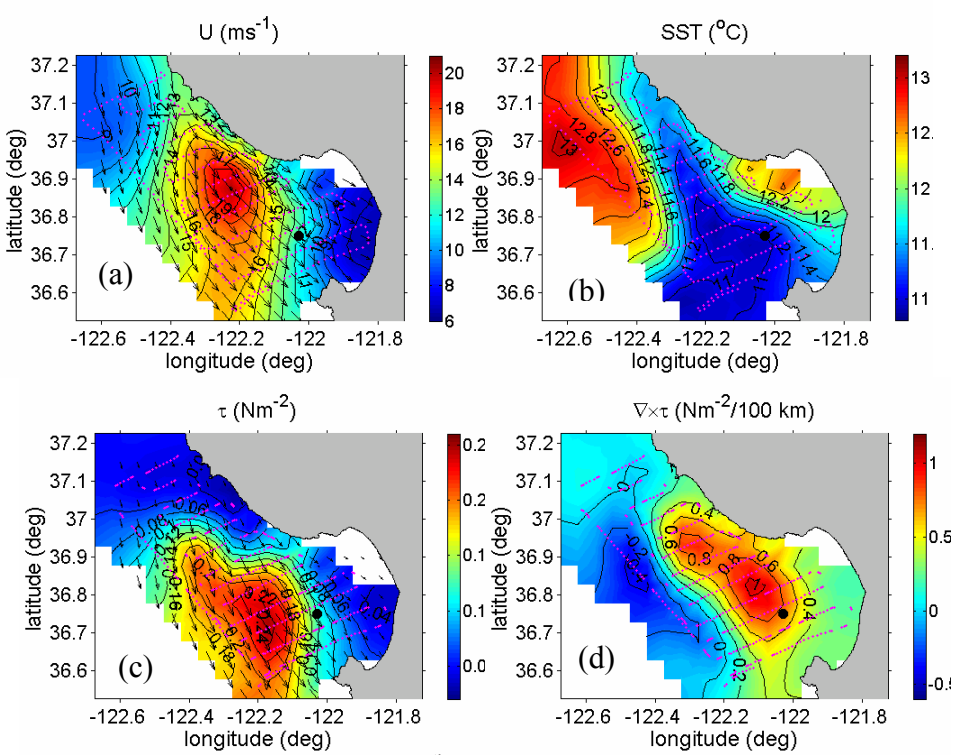

Figure 5. As in Fig. 6 but for the flight on 13th of July, 2003 from 1239 to 1657 LST with possible expansion fan to the north of Monterey Bay. The black filled circle shows the location of buoy M1.

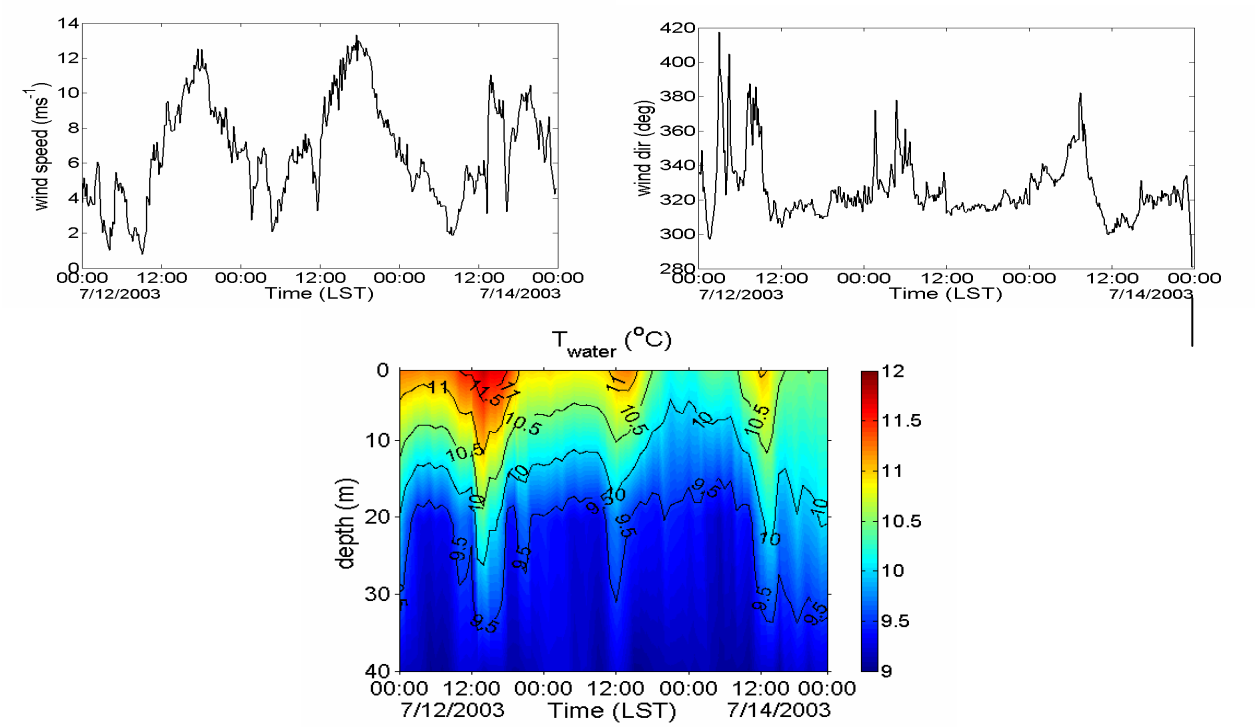

Figure 6. Variation of wind speed and direction and vertical profiles of water temperature (T_{water}) between 7/12/2003 and 7/14/2003 from buoy M1 (36.75° N, 122.03° W).

obtain with sufficient accuracy, especially at small scales. Sufficient spatial smoothing was required to reduce the random error in the estimation and made possible to analyze the variations of wind stress curl at scales larger than 15 km.

No clear correlation was seen between SST depression and wind stress curl when all data from AOSN-II were used in the analysis. Although the wind stress curl is positive and large in magnitude under northerly wind conditions, the spatial variations of stress curl were not correlated in general with SST depression. This was attributed to the complex and non-coherent small scale variations of wind stress curl as a result of relatively uniform wind field with no significant peaks. The effect of wind stress curl in the coastal zone may be reduced and spread over a broader area than far offshore or masked by background upwelling due to northerly winds which favor Ekman transport. Thus, small scale variations of wind stress curl lose correlation with SST pattern. The negative feedback of coastal upwelling on wind stress through atmospheric stability also contributes to the obscure correlation.

Similar behaviour was observed under southerly winds when wind stress curl was small and negative. In these events SST advection from persistent upwelling regions to the north and south of Monterey Bay are more significant for the formation of SST pattern in the area of the bay. On the other hand, when wind stress curl field shows coherent structures (presence of significant positive and negative centres over a relatively larger scale) in the experiment area like during onshore or offshore wind cases, a connection of wind stress curl with locally enhanced SST change was observed. The most evident effect of wind stress curl on coastal upwelling was seen when an expansion fan with significant wind speed acceleration and a peak of very high wind stress and wind stress curl occurred at the mouth of Monterey Bay.

The main conclusion from this work is that wind stress curl may result in cooling of the upper ocean through enhanced local upwelling when positive coherent features in stress curl are present over a significantly large area. Thus, concerning upwelling due to Ekman pumping only large scales need to be resolved in atmospheric and oceanic coastal models.

ACKNOWLEDGEMENTS

This work was supported by the Marine Meteorology and Atmospheric Effects program of the Office of Naval Research (ONR) award No. N0001405WR20338. S. R. Ramp's work was supported by ONR grant number N0001403WR20002 . Buoy data shown in Figure 6 were downloaded from http://aosn.mbari.org/.

REFERENCES

Brooks, I., Söderberg, S., and M. Tjernström (2003), The turbulence structure of the stable atmospheric boundary layer around a coastal headland: aircraft observations and modeling results. *Boundary-Layer Meteorol.*, **107**, 531–559.

Donelan, M.A., F.W. Dobson, S.D. Smith, and R.J. Anderson (1993), On the dependence of sea surface roughness on wave development. *J. Phys. Oceanogr.*, **23**, 2143-2149.

Dorman, C. E., Holt, T., Rogers, D.P., and K. Edwards (2000), Large-Scale Structure of the June–July 1996 Marine Boundary Layer along California and Oregon. *Mon. Wea. Rev.*, **128**, 1632–1652.

Drennan, W.M., H.C. Graber, D. Hauser, and C. Quentin (2003), On the wave age dependence of wind stress over pure wind seas. *J. Geophys. Res.*, **108**, 8062-8074.

Enriquez, A.G., and C.A. Friehe (1995), Effects of wind stress and wind stress curl variability on coastal upwelling. *J. Phys. Oceanogr.*, **25**, 1651-1671.

Enriquez, A.G., and C.A. Friehe (1997), Bulk parameterization of momentum, heat, and moisture fluxes over a coastal upwelling area. *J. Geophys. Res.*, **102**, C3, 5781-5798.

Geernaert, G. L., K. B. Katsaros, and K. Richter (1986),: Variation of the drag coefficient and its dependence on sea state. *J. Geophys. Res.*, **91**, 7667-7679.

Kalogiros, J.., and Q. Wang (2002), Calibration of a radome-differential GPS system on a Twin Otter research aircraft for turbulence measurements, *J. Atmos. Oceanic Technol.*, **19**, 159-171.

Kraus, E.B., and J.A. Businger (1994), Atmosphere-Ocean Interaction. Oxford University Press, New York.

Paduan, J. D., and L. K. Rosenfeld (1996), Remotely sensed surface currents in Monterey Bay from shore-based HF radar (CODAR), *J. Geophys. Res.*, **101**, 20,669–20,686.

Pickett, M.H., and J.D. Paduan (2003), Ekman transport and pumping in the California Current based on the U.S. Navy's high-resolution atmospheric model (COAMPS). *J. Geophys. Res.*, **108**, 3327, doi:10.1029/2003JC001902.

Ramp, S. R., Paduan, J.D., Shulman, I., Kindle, J., Bahr,F.L. and F. Chavez (2005), Observations of upwelling and relaxation events in the northern Monterey Bay during August 2000. *J. Geophys. Res.*, **110**, C07013, doi:10.1029/2004JC002538.

Rogers, D. P., Dorman, C. E., Edwards, K., Brooks, I.M., Melville, K., Burk, S. D., Thompson,W. T., Holt, T., Ström, L., Tjernström, M., Grisogono, B., Bane, J., Nuss, W., Morley, B., and A. Schanot (1998), Highlights of Coastal Waves 1996. *Bull. Amer. Meteorol. Soc.*, **79**, 1307–1326.

Rogerson, A.M. (1999), Transcritical flows in the coastal marine atmospheric boundary layer. *J. Atmos. Sci.*, **56**, 2761-2779.

Ström, L., Tjernström, M., and D.P. Rogers (2001), Observed Dynamics of Coastal Flow at Cape Mendocino during Coastal Waves 1996, *J. Atmos. Sci.*, **58**, 953-977.

Tjernström, M., and B. Grisogono (2000), Simulations of super-critical flow around points and capes in a coastal atmosphere. *J. Atmos. Sci.*, **57**, 108-135.

Winant, C.D., C.E. Dorman, C.A. Friehe and R.C. Beardsley (1988), The marine layer off the northern California. An example of supercritical flow. *J. Atmos. Sci.*, **45**, 3588-3605.

Winant, C. D., and C. E. Dorman (1997), Seasonal patterns of surface wind stress and heat flux over the Southern California Bight., *J. Geophys. Res.*, **102**, 5641– 5653.